*Stanford Exploration Project, Report 124, April 4, 2006, pages 43–**??***

Stanford Exploration Project, Report 124, April 4, 2006, pages 43–??

Selection of reference anisotropic parameters for wavefield extrapolation by Lloyd's algorithm

Yaxun Tang and Robert G. Clapp

ABSTRACT

We propose a method for selecting reference anisotropic parameters in laterally varying anisotropic media for mixed Fourier-space domain wavefield extrapolation. We treat the selection problem as a quantization procedure, and use a modified version of the 3D Lloyd's algoritm for reference-parameter selections. We demonstrate that our method yields a more accurate discription of the anisotropy model with fewer reference parameters than the uniform sampling approach. Real data examples illustrate the performance of our method.

INTRODUCTION

It is well known that wavefield-continuation-based migration methods are better able to image areas affected by multi-pathing and are more effective in handling complex wave behavior than ray-tracing-based Kirchhoff methods. However, wave-equation depth migration such as phase-shift plus interpolation (Gazdag and Sguazzero, 1984), extended split-step Fourier (Stoffa et al., 1990; Kessinger, 1992), split-step double square root (Popovici, 1996), or Fourier finite difference plus interpolation (Biondi, 2002) require multiple reference velocities for wavefield extrapolation through laterally inhomogeneous velocity models. With multiple reference velocities higher angles can be accurately handled and the quality of the image can be improved, but the cost of the migration is increased in proportion to the number of reference velocities used.

When it comes to anisotropic media, the vertical wavenumber k_z becomes a function of three anisotropic parameters (v, δ and ε (or η)). To extrapolate wavefields in Fourier domain, we must choose not only multiple reference velocities, but also multiple δs and εs (or ηs). The computational cost subsequently increases significantly. The conventional method (Rousseau, 1997; Baumstein and Anderson, 2003) for selecting those three parameters based on the geometric distribution of the input model is first to uniformly sample the vertical velocity v at each depth level, then for each vertical velocity, to uniformly sample a range of δs and ηs (or εs) from their minima to their maxima. The main drawback of this method is that it may undersample the parameters at places where the lateral variations are significant, or it may oversample the parameters at places where the model is smooth. To get a better result it may require a large number of reference parameters, which is impractical for migrating large data sets.

Clapp (2004) borrowed the idea of quantization from the field of electrical engineering, and used the 1D Lloyd's algorithm to select reference velocities for isotropic migration. He demonstrated that reference velocities selected by Lloyd's algorithm can produce higher-quality images while using fewer reference velocities. In fact, the 1D Lloyd's algorithm (Lloyd, 1982) is a special case of the clustering method, which tries to find the global optimum solutions according to some statistical criteria. Reference-velocity selection based on the statistical distribution of the velocity model is receiving increasing attention (Bagaini et al., 1995; Geiger and Margrave, 2005). In the companion paper, Clapp (2006) extends the 1D Lloyd's algorithm to multi-dimensional case, and in this paper we use the 3D version of Lloyd's algorithm to select the reference anisotropic parameters for wavefield extrapolation in laterally varying VTI media. We show that, by incorporating the 3D Lloyd's algorithm, we greatly reduce the computational cost and obtain high-quality images.

GENERALIZED LLOYD'S ALGORITHM

The concept of quantization originates in the field of electrical engineering. The basic idea behind quantization is to describe a continuous function, or one with a large number of samples, by a few representative values. Let x denote the input signal and $\hat{x} = Q(x)$ denote quantized values, where $Q(\cdot)$ is the quantizer mapping function. There will certainly be a distortion if we use $\hat{x}$ to represent x. In the least-square sense, the distortion can be measeured by

$$D = \int_{-\infty}^{\infty} (x - Q(x))^2 f(x) dx, \tag{1}$$

where $f(x)$ is the probability density function of the input signal. Consider the situation with L quantizers $\hat{x} = (\hat{x}_1, \hat{x}_2, \cdots, \hat{x}_L)$. Let the corresponding quantization intervals be

$$T_i = (a_{i-1}, a_i), i = 1, 2, \ldots, L, \tag{2}$$

where $a_0 = -\infty$ and $a_L = \infty$. Then

$$D = \int_{-\infty}^{\infty} (x - Q(x))^2 f(x) dx = \sum_{i=1}^{L} \int_{T_i} (x - \hat{x}_i)^2 f(x) dx. \tag{3}$$

In the discrete case, equation (3) can be written as follows:

$$D = \sum_{i=1}^{L} \sum_{x=a_{i-1}}^{a_i} P(x)(x - \hat{x}_i)^2, \tag{4}$$

where $P(x)$ is the discrete version of the probability density function, or normalized histogram ($\sum_x P(x) = 1$). To minimize the distortion function D, we take derivatives of equation (4) with respect to $\hat{x}_i$, a_i and set them equal to zero, leading to the following conditions for the optimum quantizers $\hat{x}_i$ and quantization interval boundaries $\hat{a}_i$:

$$\hat{a}_i = \frac{\hat{x}_i + \hat{x}_{i+1}}{2}, \tag{5}$$

$$\hat{x}_i = \frac{\sum_{x=\hat{a}_{i-1}}^{\hat{a}_i} P(x) x}{\sum_{x=\hat{a}_{i-1}}^{\hat{a}_i} P(x)}. \tag{6}$$

A way to solve this coupled set of nonlinear equations is to first generate an initial set $\{x_1, x_2, \ldots, x_L\}$, then apply equations (5) and (6) alternately until convergence is obtained. This iteration is well known as the Lloyd-Max quantization algorithm (LMQ).

It is fairly straightforward to extend the LMQ to 3D. The main extension of the approach is to break the input data points into 3D clusters instead of 1D cells. A 1D normalized histogram should be replaced with a 3D normalized histogram and a 3D distortion function should be calculated as follows:

$$D = \sum_{m=1}^{L} \left(\sum_{x=a_{i-1}}^{a_i} \sum_{y=b_{j-1}}^{b_j} \sum_{z=c_{k-1}}^{c_k} P(x,y,z)(\mathbf{r}-\hat{\mathbf{r}}) \cdot (\mathbf{r}-\hat{\mathbf{r}}) \right), \tag{7}$$

where $\hat{\mathbf{r}} = (\hat{x}_m, \hat{y}_m, \hat{z}_m)$ is the center of cluster m, $P(x,y,z)$ is the 3D histogram at point $\mathbf{r} = (x,y,z)$ within cluster m, and $(a_{i-1}, a_i), (b_{j-1}, b_j), (c_{k-1}, c_k)$ define the boundaries of cluster m. Conditions (5) and (6) accordingly become:

1. Classification of the points. The Euclidian distance between a point and every cluster center (i.e. quantizer) is calculated. The point is assigned to the closest cluster center.
2. Updating of the quantizers. Each quantizer is the center of mass of all points which are assigned to the cluster.

It should be pointed out that LMQ is highly dependent on the initial solution and can easily get stuck in local minima. One simple but effective way to avoid these problems is to start with a uniform quantizer, and when a cluster becomes empty, replace it by splitting regions with high variance (Clapp, 2004). The detailed implementation of the modified 3D Lloyd's algorithm is discussed by Clapp (2006).

SELECTING REFERENCE ANISOTROPIC PARAMETERS

Anisotropy has been shown to exist in many sedimentary rocks (Thomsen, 1986). Most sedimentary rocks can be approximated by a transversely isotropic medium with a plane of symmetry. For vertically transversely isotropic (VTI) media, if we assume that the S-wave velocity is much smaller than the P-wave velocity, the dispersion relation can be computed as follows (Tsvankin, 2001):

$$k_z(v,\delta,\eta) = \frac{\omega}{v}\sqrt{\frac{\frac{\omega^2}{v^2} - k_x^2(1+2\varepsilon)}{\frac{\omega^2}{v^2} - 2k_x^2\eta(1+2\delta)}}, \tag{8}$$

$$\eta = \frac{\varepsilon - \delta}{1+2\delta}, \tag{9}$$

where v, δ, ε (and η) are the anisotropic parameters (Thomsen, 1986; Tsvankin, 2001). In the VTI media, the vertical wavenumber k_z is a function not only of vertical velocity v, but also of δ and η (or ε), which means that for one depth-level extrapolation, we must choose three parameters instead of one.

The 3D Lloyd's algorithm can be easily translated into the problem of selecting reference anisotropic parameters, because these three anisotropic parameters are always correlated and have similar distributions. These properties make the selection by Lloyd's algorithm quite effective. In our selection problem, we form the parameter vector $\mathbf{r} = (v, \delta, \eta)$ or $\mathbf{r} = (v, \delta, \varepsilon)$. Now the center of the 3D mass within a cluster is the reference-parameter vector $\hat{\mathbf{r}}$, and the boundaries of the 3D cluster define the regions with the same v, δ and η (or ε).

We test our methodology on a real data set provided by ExxonMobil. Figure 1 displays the corresponding anisotropy model also provided by ExxonMobil. Figure 1(a) is the vertical velocity model, Figure 1(b) is the δ model and Figure 1(c) is the η model. As the 3D Lloyd's algorithm is hard to visualize, we show only a 2D procedure for selecting δ and η. Figures 2(a) and 2(b) are the input δ and η for a single depth level respectively. Figure 2(c) is their 2D histogram, where the horizontal axis is η, the vertical axis is δ, and the amplitude is the value of the 2D histogram. Figure 3(a) shows the result by regular sampling, where 16 uniformly-selected points (4 δs and 4 ηs) are overlaid with the 2D histogram (Figure 2(c)). It is quite clear that the points selected by regular sampling do not match well the distribution of δ and η. Figure 3(b) shows the result by using the modified Lloyd's alogrithm after 2 iterations, while Figure 3(c) is the result after 20 iterations. Note how well the result characterizes the 2D distribution of δ and η, and also note that after 20 iterations the number of (δ, η) is reduced from 16 to 10. Thus for this depth level and a given vertical velocity, we only need 10 depth extrapolations instead of 16, reducing the computational cost by almost 40 percent.

MIGRATION RESULTS

To compare the migration results we uniformly select three vs, δs and ηs separately for the conventional method; the chosen reference parameters are shown in Figure 4. For the modified 3D Lloyd's method, we also start with three vs, three δs and three ηs as the initial input and we set the maximum number of anisotropic parameters equal to 27 for each depth level. This guarantees that the number of parameters selected by the modified 3D Lloyd's algorithm will be no larger than that obtained by uniform sampling. In this case, the total number of depth levels is $nz = 410$; hence, for a uniform sampling of reference parameters, we must perform $410 \times 27 = 11070$ wavefield extrapolations. After selecting by the modified Lloyd's algorithm, however, the total number of extrapolations reduces to 4952, reducing the computation time by about 54%. Figure 5 illustrates the reference parameters selected by the modified 3D Lloyd's algorithm. It is clear in Figure 5 that Lloyd's algorithm has done a very good job of describing the actual model. Figures 6–8 show the error maps between the actual model and the selected reference parameters both by the conventional method and the modified 3D Lloyd's method. Obviously, using Lloyd's method, we obtain much smaller differences between the actual model and the reference parameters.

Figure 9(a) shows the anisotropic prestack migration result of the conventional approach, while Figure 9(b) shows the result of using the modified 3D Lloyd's algorithm for reference-

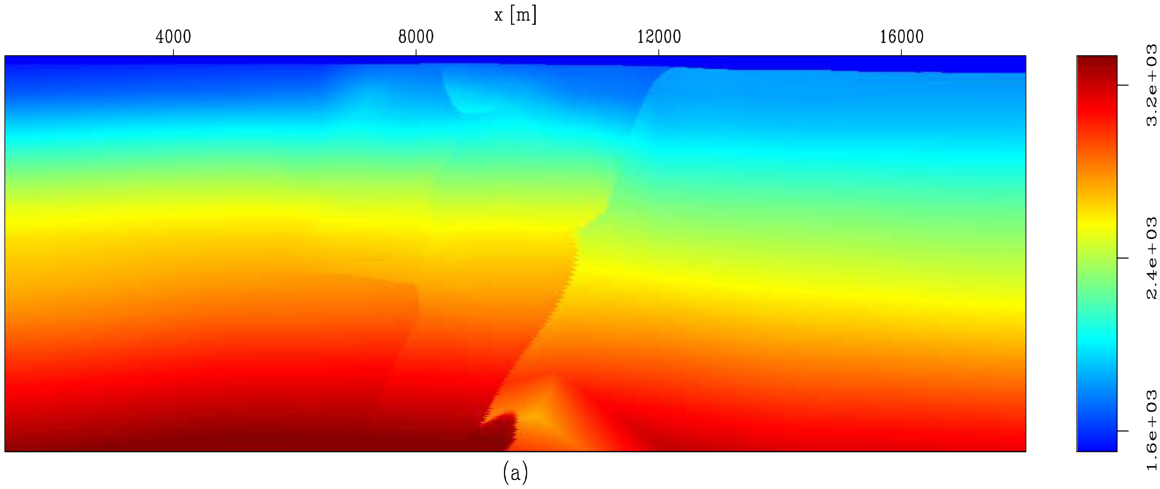

(a)

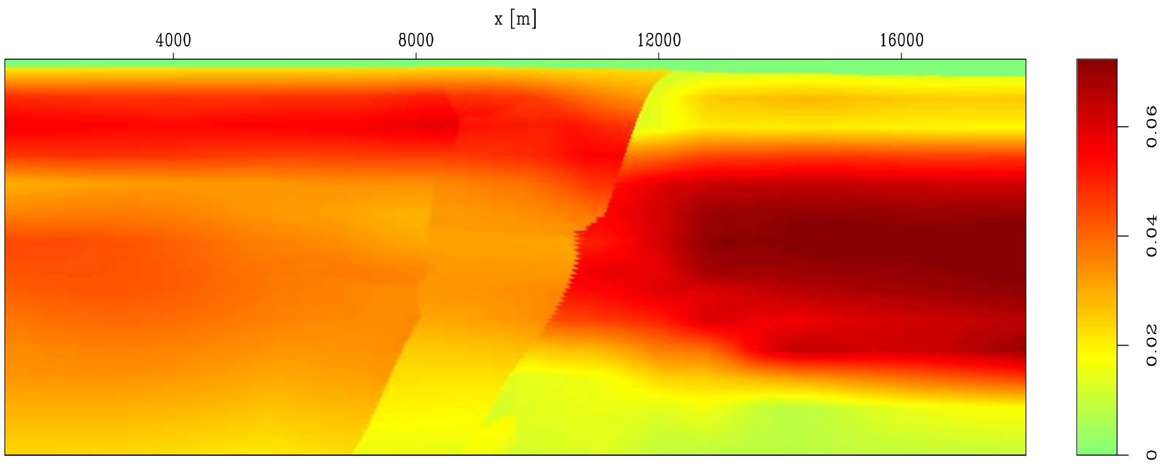

(b)

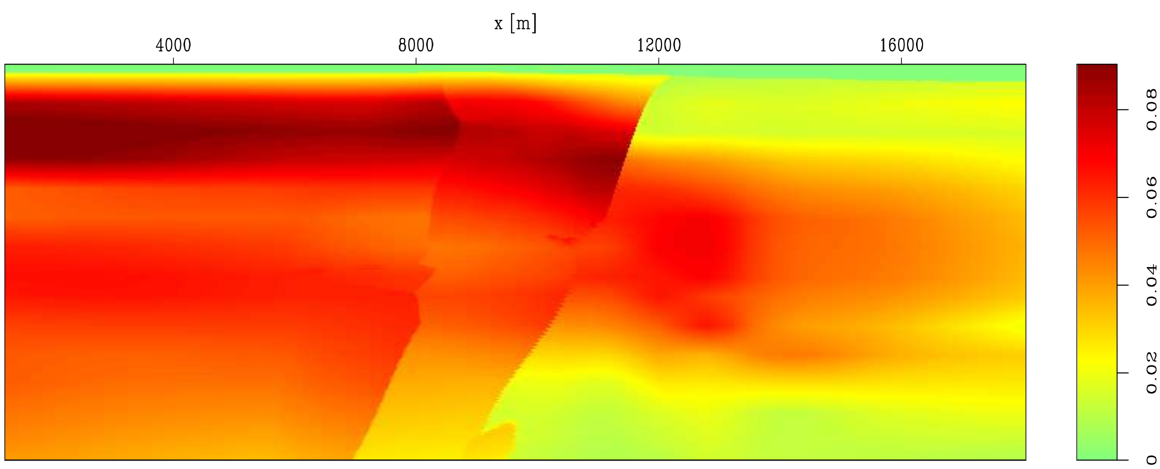

(c)

Figure 1: Vertical slice of the anisotropy model provided by ExxonMobil (the vertical axes are depths). (a) P-wave velocity; (b) anisotropic parameter δ and (c) anisotropic parameter η. yaxun1-model [ER]

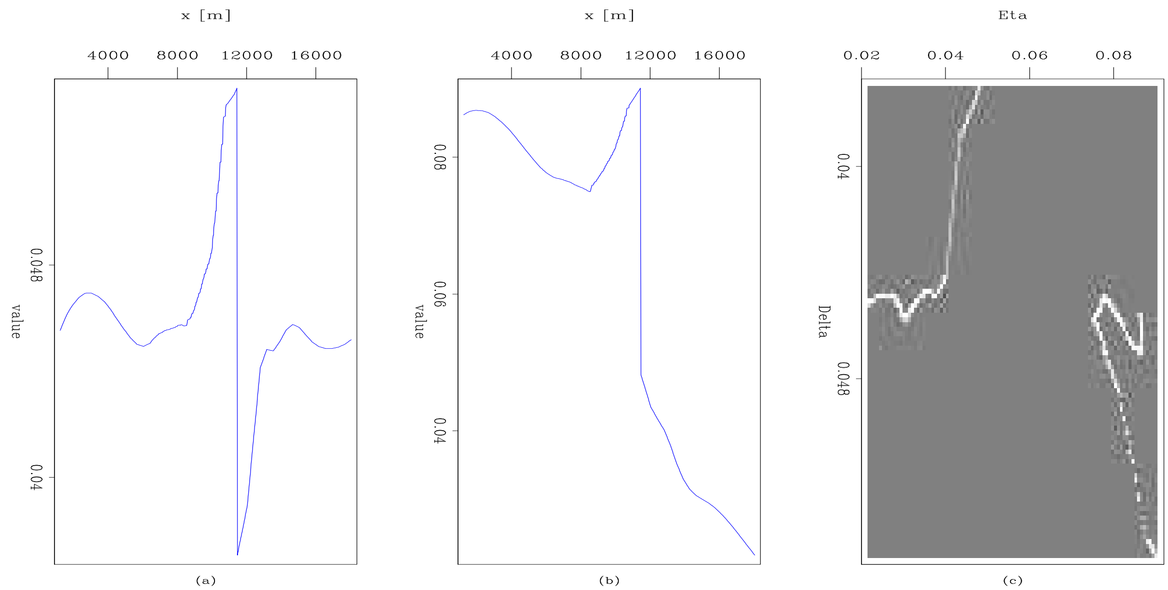

Figure 2: The values of δ, η for a single depth slice and their 2D histogram. The values of (a) δ at depth=990m and (b) η at depth=990m; (c) the 2D histogram computed from (a) and (b), the curves indicate the 2D distribution of δ and η. yaxun1-2D_histogram [ER]

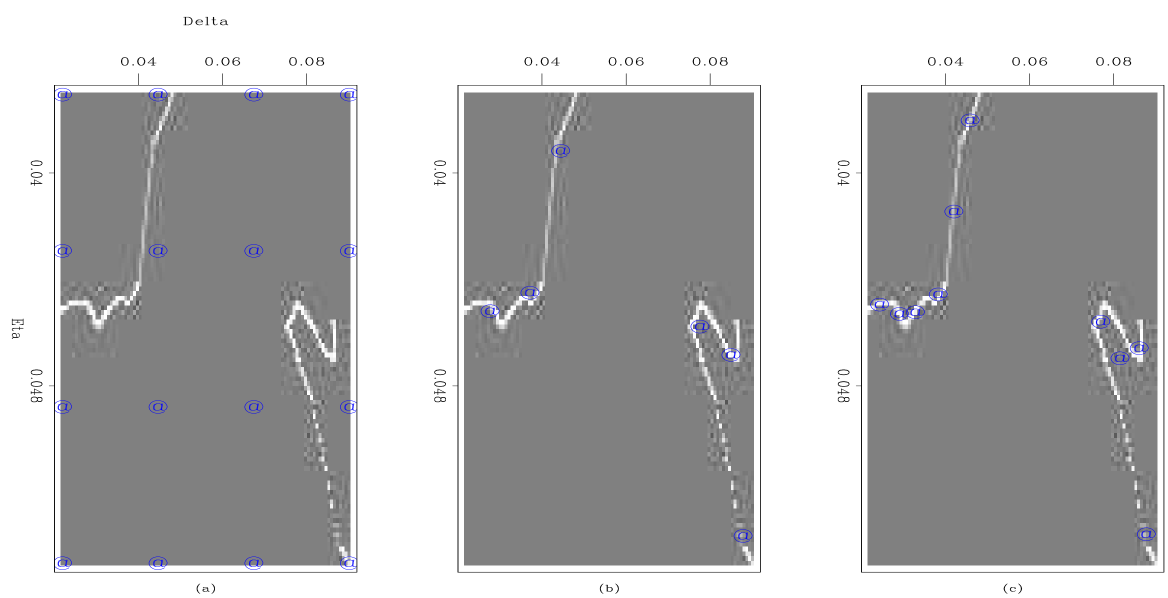

Figure 3: Comparison between the conventional method and the modified 2D Lloyd's algorithm. (a) The result of uniform sampling, overlaid with the 2D histogram from Figure 2(c); (b) the result of the modified 2D Lloyd's algorithm after 2 iterations and (c) after 20 interations. Note how accurately (b) and (c) characterize the distribution of δ and η yaxun1-overlay_lloyd [ER]

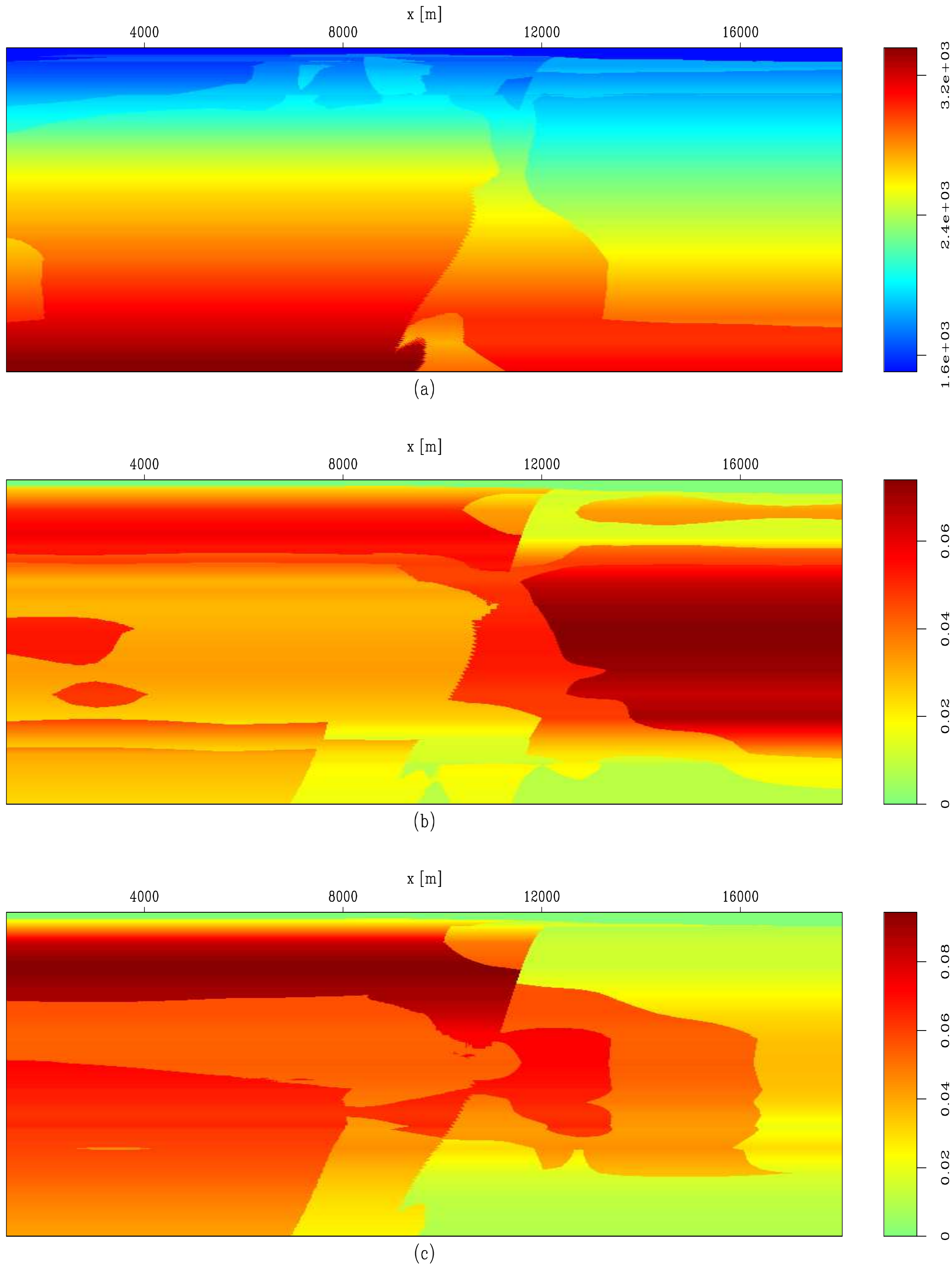

Figure 4: Selection of anisotropic parameters by uniform sampling (the vertical axes are depths). (a) Reference velocity; (b) reference δ; (c) reference η. yaxun1-para_uniform [ER]

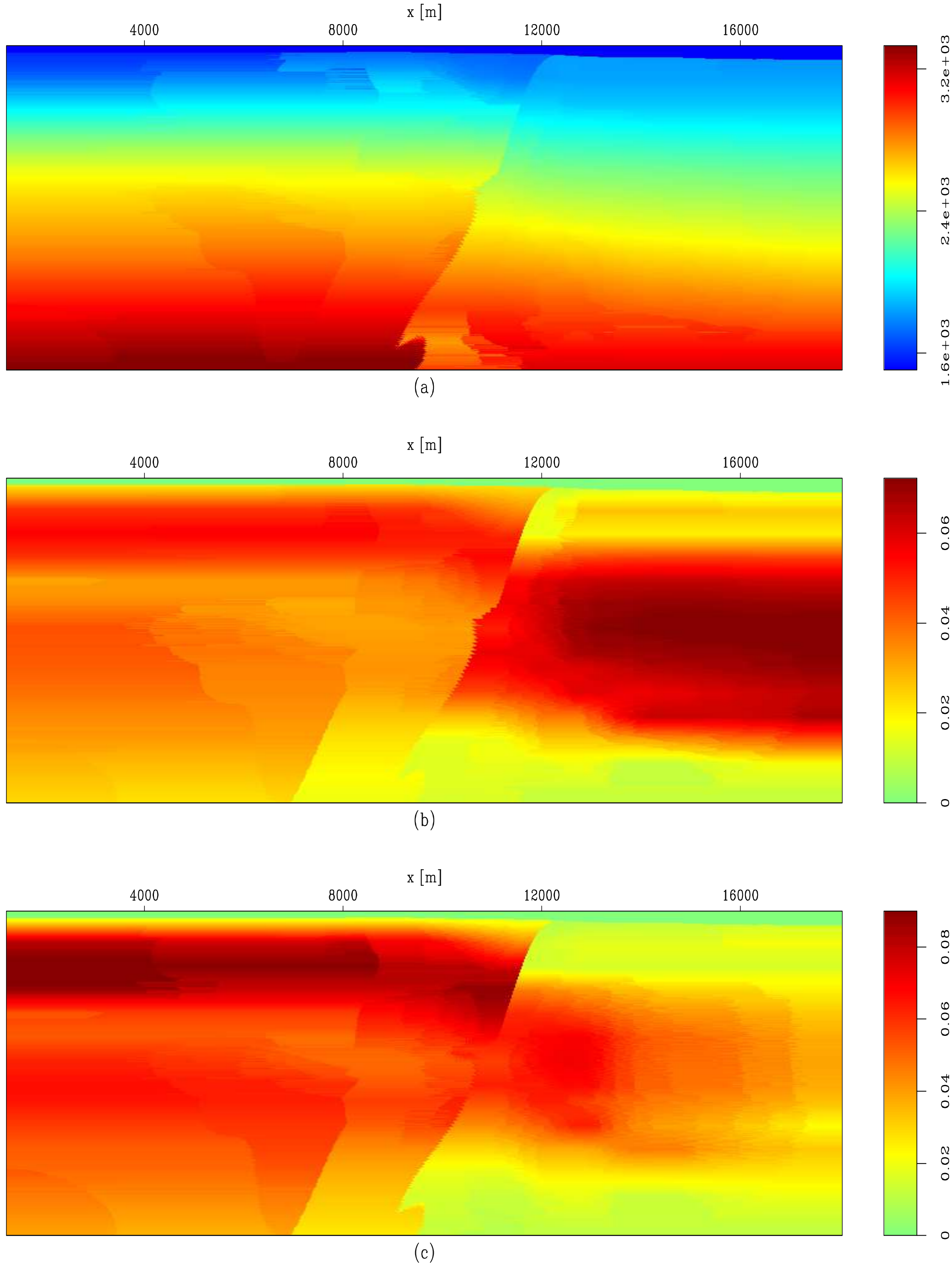

Figure 5: Selection of anisotropic parameters by the modified 3D Lloyd's algorithm (the vertical axes are depths). (a) Reference velocity; (b) reference δ; (c) reference η. yaxun1-para_lloyd [ER]

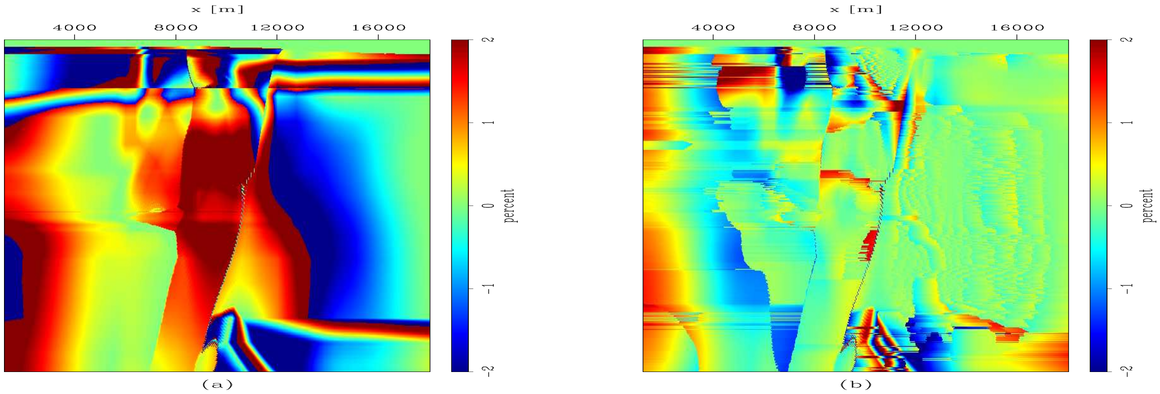

Figure 6: Error map between the actual velocities and the reference velocities (the vertical axes are depths). Both maps are shown in the same scale (percentage). (a) By conventional method; (b) by Lloyd's algorithm. yaxun1-error_pv [ER]

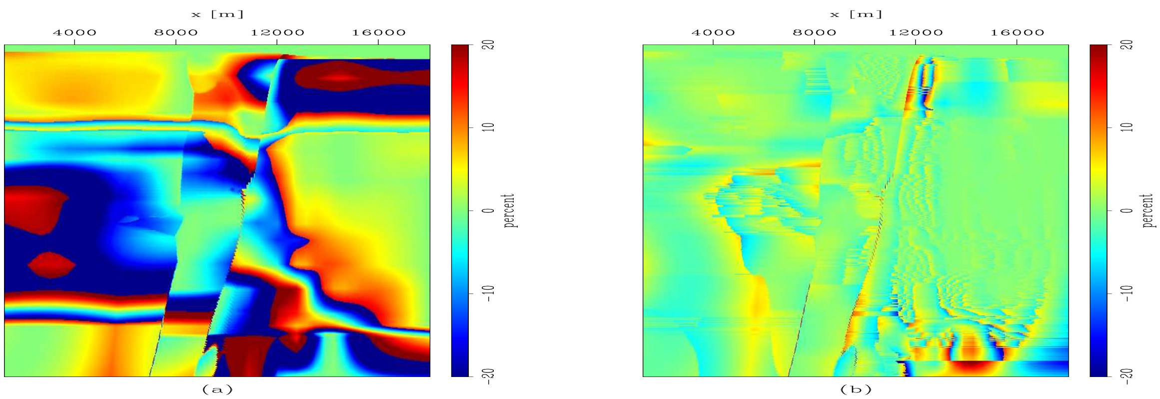

Figure 7: Error map between the actual δ and the reference δ (the vertical axes are depths). Both maps are shown in the same scale (percentage). (a) By conventional method; (b) by Lloyd's algorithm. yaxun1-error_delta [ER]

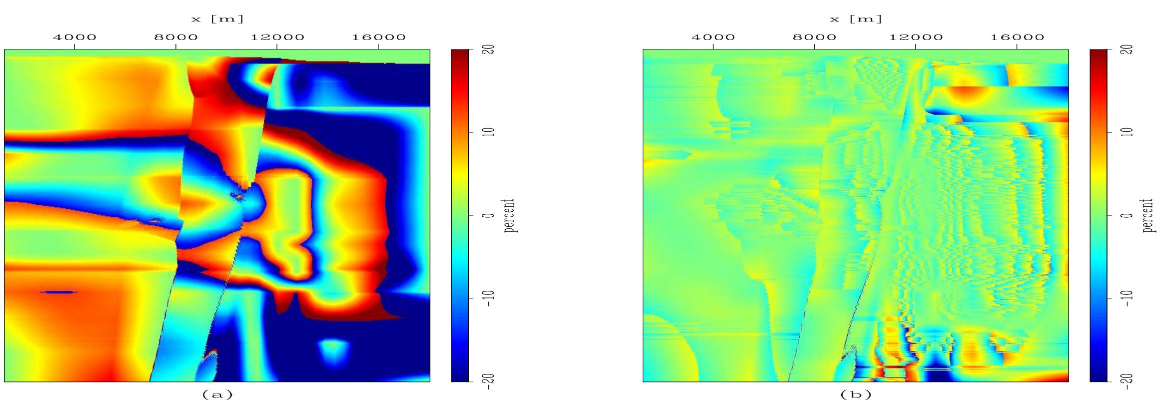

Figure 8: Error map between the actual η and the reference η (the vertical axes are depths). Both maps are shown in the same scale (percentage). (a) By conventional method; (b) by Lloyd's algorithm. yaxun1-error_eta [ER]

parameter selections. Though in both cases, all reflectors are nicely imaged, we can still identify the differences between Figure 9(a) and 9(b). Using the modified 3D Lloyd's algorithm yields a more focused and continuous salt flank (portion B); the layers, especially A and C, have stronger amplitudes and are better imaged. The angle-domain common image gathers (ADCIGs) for different surface locations computed from images obtained by using both methods are illustrated next to each other in Figure 10 . Figures 10(a), 10(c) and 10(e) are the ADCIGs computed from the image obtained by using the uniform sampling method (Figure 9(a)) at surface location $x = 5,875$ meters, $11,375$ meters and $13,875$ meters respectively, while Figures 10(b), 10(d) and 10(f) are the corresponding ADCIGs from the image obtained by using the modified Lloyd's algorithm (Figure 9(b)) at surface location $x = 5,875$ meters, $11,375$ meters and $13,875$ meters respectively. The differences between the ADCIGs computed from Figure 9(a) and those computed from Figure 9(b) are minor, but we can still see that the ADCIGs shown in Figures 10(b), 10(d) and 10(f) are generally more flat and continuous than those illustrated in Figures 10(a), 10(c) and 10(e), which indicates that the reference anisotropic parameters selected by the modified 3D Lloyd's algorithm are more accurate than those selected by the uniform sampling method. One thing needed for an extra emphasis is that the computational cost by using Lloyd's algorithm is only half of that by using the conventional method.

CONCLUSION

By extending the 1D Lloyd's algorithm to 3D, we have presented a method for selecting reference anisotropic parameters for wavefield downward continuation. The modified Lloyd's algorithm is a dynamic process that automatically determines the fewest reference parameters necessary to best characterize the actual model for each depth level. It eliminates reference parameters that are redundant or contribute little to the result. Therefore, by using the modified Lloyd's algorithm, it is possible for us to obtain an optimum migration result with relatively few reference parameters, greatly reducing the computational cost compared with the conventional method. Our test on real data shows that reference anisotropic parameters selected by the modified 3D Lloyd's algorithm characterize the actual model well, and that migrating with those reference parameters leads to an image with higher quality, at lower cost, than the conventional selection method.

ACKNOWLEDGMENTS

We would like to thank ExxonMobil Exploration Company for making the data set available for SEP through the generous efforts of Ruth Gonzalez and Joe Reilly. The corresponding anisotropy models were kindly shared with us by Laura Bear and Jerry Krebs, also at ExxonMobil.

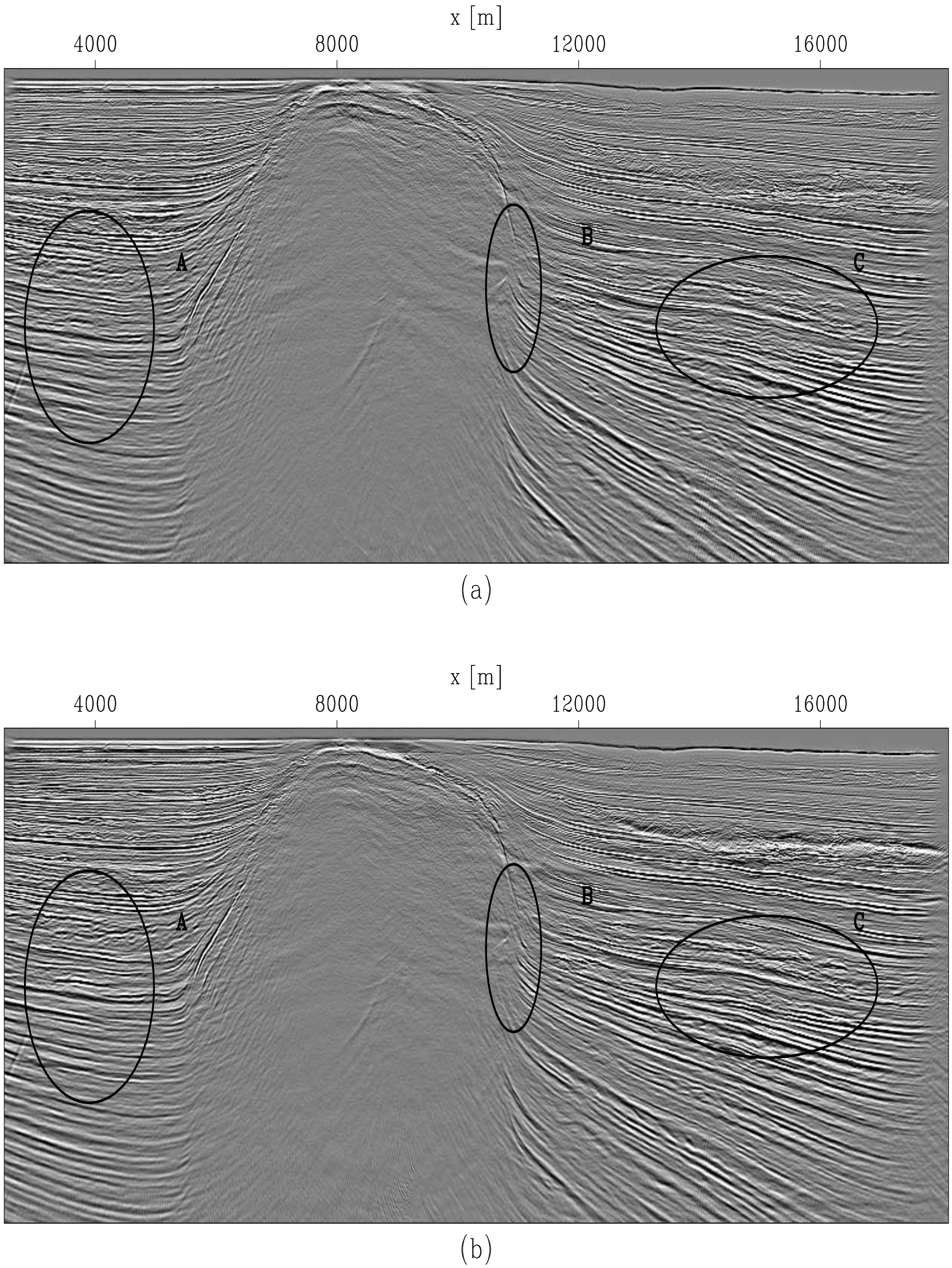

Figure 9: Anisotropic prestack migration result (the vertical axes are depths). (a) Reference parameters selected by the conventional method; (b) reference parameters selected by the modified 3D Lloyd's algorithm. The computational cost for (b) is only half of that for (a) yaxun1-animig [CR]

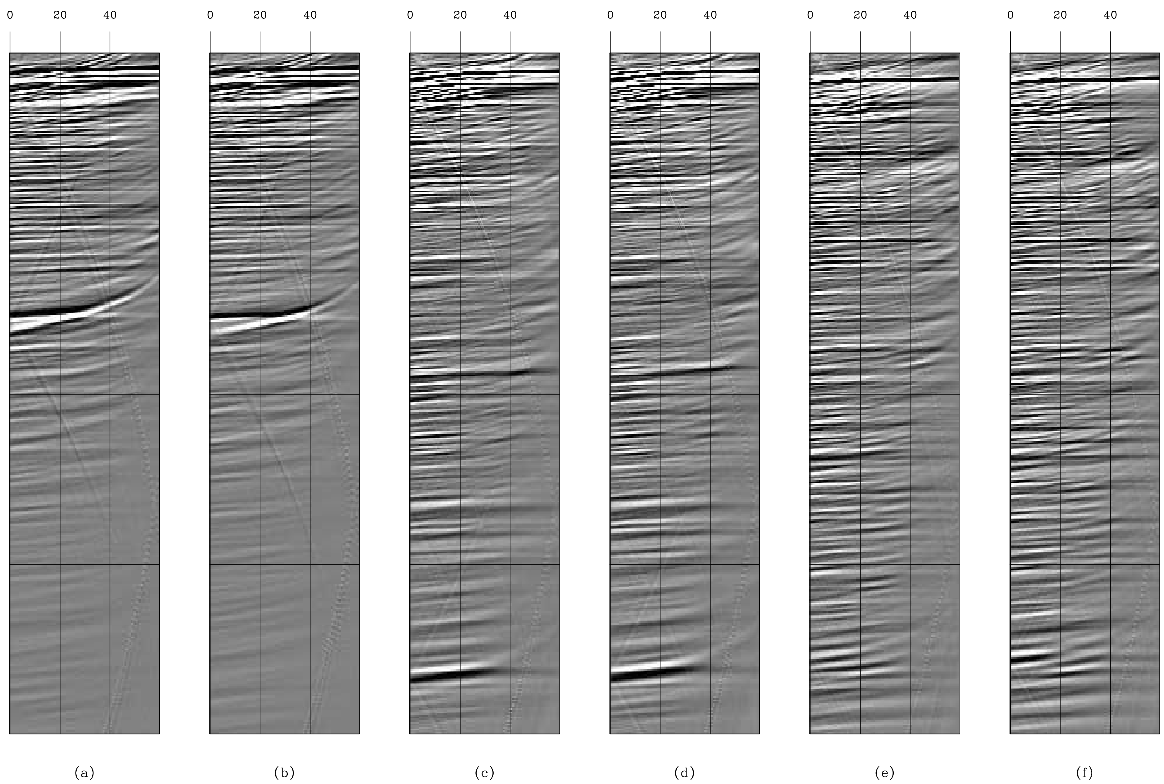

Figure 10: ADCIGs for different surface locations (the vertical axes are depths, while the horizontal axes are angles). (a), (c) and (e) are ADCIGs computed from the migration result obtained by using uniform sampling at horizontal locations $x = 5,875$ meters, $11,375$ meters and $13,875$ meters respectively, while (b), (d) and (f) are ADCIGs computed from the migration result obtained by using the modified 3D lloyd's algorithm at horizontal locations $x = 5875$ meters, $11,375$ meters and $13,875$ meters respectively. yaxun1-anglegather [CR]

REFERENCES

Bagaini, C., Bonomi, E., and Pieroni, E., 1995, Data parallel implementation of 3-D PSPI *in* 65th Ann. Internat. Mtg. Soc. of Expl. Geophys., 188–191.

Baumstein, A., and Anderson, J. E., 2003, Wavefield extrapolation in laterally varying vti media: 73rd Ann. Internat. Mtg., Soc. of Expl. Geophys., Expanded Abstracts, 945–948.

Biondi, B., 2002, Stable wide-angle Fourier finite-difference downward extrapolation of 3-D wavefields: Geophysics, **67**, 872–882.

Clapp, R. G., 2004, Reference velocity selection by a generalized lloyd method: 74th Ann. Internat. Mtg., Soc. of Expl. Geophys., Expanded Abstracts, 981–984.

—, 2006, A modified lloyd algorithm for characterizing vector fields: SEP– **124**.

Gazdag, J., and Sguazzero, P., 1984, Migration of seismic data by phase-shift plus interpolation: Geophysics, **49**, 124–131.

Geiger, H. D., and Margrave, G. F., 2005, Automatic selection of reference velocities for recursice depth migration by peak search method: 75th Ann. Internat. Mtg., Soc. of Expl. Geophys., Expanded Abstracts, 2056–2059.

Kessinger, W., 1992, Extended split-step Fourier migration *in* 62nd Ann. Internat. Mtg. Soc. of Expl. Geophys., 917–920.

Lloyd, S. P., 1982, Least squares quantization in pcm: IEEE Transactions on Information Theory.

Popovici, A. M., 1996, Prestack migration by split-step DSR: Geophysics, **61**, 1412–1416.

Rousseau, J. H. L., 1997, Depth migration in heterogeneous, transversely isotropic media with the phase-shift-plus-interpolation method *in* 67th Ann. Internat. Mtg. Soc. of Expl. Geophys., 1703–1706.

Stoffa, P. L., Fokkema, J. T., de Luna Freire, R. M., and Kessinger, W. P., 1990, Split-step Fourier migration: Geophysics, **55**, 410–421.

Thomsen, L., 1986, Weak elastic anisotropy: Geophysics, **51**, 1954–1966.

Tsvankin, I., 2001, Seismic signatures and analysis of reflection data in anisotropic media: Pergamon.